



Experiment Report Form

The double page inside this form is to be filled in by all users or groups of users who have had access to beam time for measurements at the ESRF.

Once completed, the report should be submitted electronically to the User Office via the User Portal:
<https://www.esrf.fr/misapps/SMISWebClient/protected/welcome.do>

Deadlines for submission of Experimental Reports

Experimental reports must be submitted within the period of 3 months after the end of the experiment.

Experiment Report supporting a new proposal (“relevant report”)

If you are submitting a proposal for a new project, or to continue a project for which you have previously been allocated beam time, you must submit a report on each of your previous measurement(s):

- even on those carried out close to the proposal submission deadline (it can be a “*preliminary report*”),
- even for experiments whose scientific area is different from the scientific area of the new proposal,
- carried out on CRG beamlines.

You must then register the report(s) as “relevant report(s)” in the new application form for beam time.

Deadlines for submitting a report supporting a new proposal

- 1st March Proposal Round - **5th March**
- 10th September Proposal Round - **13th September**

The Review Committees reserve the right to reject new proposals from groups who have not reported on the use of beam time allocated previously.

Reports on experiments relating to long term projects

Proposers awarded beam time for a long term project are required to submit an interim report at the end of each year, irrespective of the number of shifts of beam time they have used.

Published papers

All users must give proper credit to ESRF staff members and proper mention to ESRF facilities which were essential for the results described in any ensuing publication. Further, they are obliged to send to the Joint ESRF/ ILL library the complete reference and the abstract of all papers appearing in print, and resulting from the use of the ESRF.

Should you wish to make more general comments on the experiment, please note them on the User Evaluation Form, and send both the Report and the Evaluation Form to the User Office.

Instructions for preparing your Report

- fill in a separate form for each project or series of measurements.
- type your report in English.
- include the experiment number to which the report refers.
- make sure that the text, tables and figures fit into the space available.
- if your work is published or is in press, you may prefer to paste in the abstract, and add full reference details. If the abstract is in a language other than English, please include an English translation.



	Experiment title: Emergent phenomena between the <i>CE</i> -type and <i>G</i> -type orbital ordered ground states of $\text{Hg}_{1-x}\text{Na}_x\text{Mn}_3\text{Mn}_4\text{O}_{12}$	Experiment number: HC-5203
Beamline: ID22	Date of experiment: from: 29/06/23 to: 03/07/23	Date of report:
Shifts: 9	Local contact(s): Ola gjonnes Grendal	<i>Received at ESRF:</i>
Names and affiliations of applicants (* indicates experimentalists): Dr Mark Senn¹, Dr Wei-tin Chen^{2-3,*}, Dr Struan Simpson^{1,*}, Dr Catriona Crawford^{1,*}, Mr Benjamin Tragheim^{1,*}, Miss En-Pei Liu^{2,*} ¹ Department of Chemistry, University of Warwick, Gibbet Hill, Coventry, CV4 7AL, UK ² Centre for Condensed Matter Sciences and Center of Atomic Initiative for New Materials, National Taiwan University, Taipei 10617, Taiwan ³ Taiwan Consortium of Emergent Crystalline Materials of Science and Technology, Taipei 10622, Taiwan		

Report:

The colossal magnetoresistance (CMR) in manganite perovskites has been extensively investigated, with the key regime identified around $x = 3/8$ in $\text{La}_{1-x}\text{Ca}_x\text{MnO}_3$ (LCMO) to exhibit maximum MR effect. However, complications of the LCMO system associated with electronic phase separation have prevented an atomistic-level understanding of the lattice, charge and orbital degrees of freedom in the phase diagram. Recently, we have used a prototype $\text{AMn}^A_3\text{Mn}^B_4\text{O}_{12}$ quadruple perovskite ($A = \text{Na}_{1-x}\text{Ca}_x$ and $\text{La}_{1-x}\text{Ca}_x$), prepared with high pressure synthesis techniques, to tackle this issue.¹ With high resolution synchrotron x-ray diffraction data obtained from ID22 and detailed crystallographic analysis, a compositional phase diagram, showing the evolution of the distortion modes associated with the various kinds of orbital order (OO), was obtained. A new kind of OO was revealed at the critical doping level $\text{Na}_{0.4}\text{Ca}_{0.6}\text{Mn}_3\text{Mn}_4\text{O}_{12}$ ($\text{Mn}^B \sim \text{Mn}^{+3.375}$) consisting of orbital ordered and charge disordered stripes. Such a phase provides the missing intermediate states between *C*-type orbital order ($\text{Mn}^B = \text{Mn}^{3+}$, $A = \text{La}$) and the *CE*-type charge and OO ($\text{Mn}^B = \text{Mn}^{3.5+}$, $A = \text{Na}$) insulating phase, from which CMR is thought to emerge.

On the other hand, we have found related $\text{HgMn}_3\text{Mn}_4\text{O}_{12}$ (HMO) to exhibit a polar ground state on account of charge transfer, between *A* and *B* sites, followed by *G*-type charge and orbital order on the *B*-sub lattice at low temperature.² Such behavior was not observed in the $\text{CaMn}_3\text{Mn}_4\text{O}_{12}$ analogue, which forms instead an intermediate *C*-type orbital ordered structure with rhombohedral symmetry. This indicates that the mercury cation (Hg^{2+} with filled $5d^{10}$ orbital) plays a crucial role in the intertwined charge, orbital and spin coupling and the physical properties of HMO. These $\text{AMn}^A_3\text{Mn}^B_4\text{O}_{12}$ thus show an even richer orbital and charge ordered physics than their canonical LCMO counterparts.

To investigate more fully how the precise pattern of charge and orbital ordering, and hence properties, can be tuned in these fascinating materials, we have synthesised the novel series of materials $\text{Hg}_{1-x}(\text{La,Ca,Na})_x\text{Mn}_3\text{Mn}_4\text{O}_{12}$, with single chemical substitution of either La, Ca, Na for Hg at the *A*-site, under high

pressure conditions. The substitution results in not only the tuning of the charge on the B -site, but also the unique series of structural phase transitions observed across the series. Therefore, in order to resolve the weak superstructure peaks, monoclinic and tetragonal pseudo-symmetry-breaking distortions in these materials that are associated with their different orbital ordered states, the high resolution data obtained by ID22 was required.

High resolution synchrotron powder X-ray diffraction data were collected in the temperature range $10 \text{ K} \leq T \leq 300 \text{ K}$ for the compositions in the series $\text{Hg}_{1-x}(\text{La}, \text{Ca}, \text{Na})_x\text{Mn}_3\text{Mn}_4\text{O}_{12}$ ($0 < x \leq 0.5$), with representative datasets at 300 K and 10 K shown in Figures 1 and 2. For the Na substituted series, at 300 K the evolution of rhombohedral to cubic space group symmetries is observed as a function of Na composition at a critical point of $x = 0.3$ (Figure 1). Furthermore, in comparison to the datasets collected at 10 K a temperature-induced phase transition from rhombohedral to orthorhombic symmetries is observed for compositions in the range $0.05 \leq x \leq 0.3$, while for the higher substitutions it is likely that a cumulation of cubic, orthorhombic and monoclinic phases are present. For the La-substituted series, rhombohedral symmetry is preserved as a function of composition at 300 K, as shown in Figure 2. Upon cooling to 10 K, orthorhombic symmetry is rapidly suppressed as a function of composition. Preliminary Rietveld refinements for the $x = 0.05$ and 0.10 compositions indicate both rhombohedral and orthorhombic phases emerge upon cooling to 10 K (Figure 2), while for $x \geq 0.15$ only the rhombohedral phase is present.

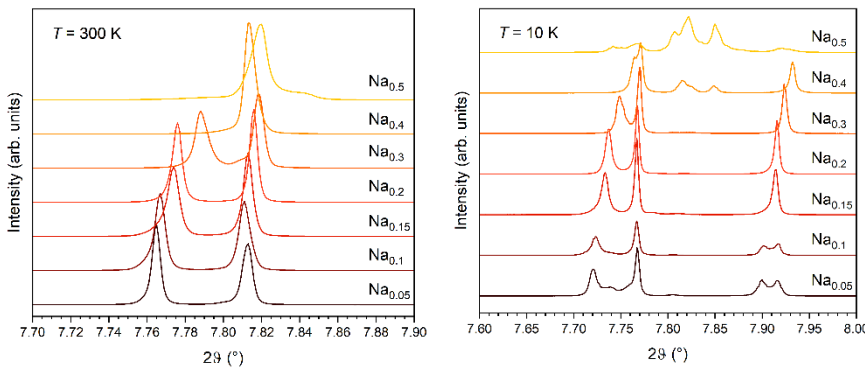


Figure 1: Compositional evolution of peak splitting at $T = 300 \text{ K}$ (left) and 10 K (right). Confirmed by Rietveld refinements, rhombohedral $R\bar{3}$ ($0.05 \leq x \leq 0.3$) and cubic $Im\bar{3}$ ($x = 0.4, 0.5$) space groups are observed at 300 K. At 10 K, respective compositions undergo an $R\bar{3}$ to $Pnn2$ phase transition, while for $x = 0.4$ and 0.5 the phase transition is less clear, adopting cumulations of cubic, monoclinic, and orthorhombic phases.

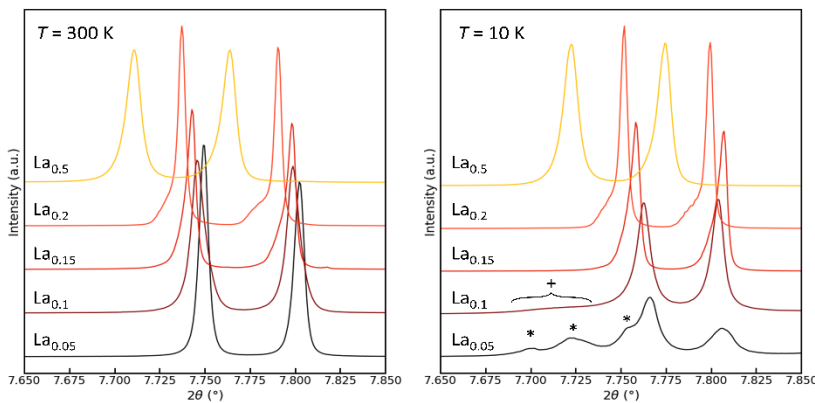


Figure 2: Compositional evolution of peak splitting at $T = 300 \text{ K}$ (left) and 10 K (right). Asterisks mark distinguishable $Pnn2$ reflections in the $x = 0.05$ dataset, while the “+” symbol denotes highly strained $Pnn2$ reflections present in the $x = 0.10$ pattern (confirmed by Rietveld refinement).

Next steps in the data analysis for these datasets includes the optimisation of Rietveld refinements of various structural models used to describe the rich orbital ordering regimes present in the quadruple manganite perovskites. Additionally, datasets with compositions involving Ca-substitution will be further investigated once the Na and La series have been more fully mapped, whereby signatures of incommensurability are present in this series and not in the latter two series. Furthermore, by using the symmetry-motivated basis of irreducible representation analysis, the evolution of the distortion modes controlling the emergence of the different orbital ordered states will be systematically tracked as a function of temperature and composition. This will then provide mechanistic insight into how the different orbital regimes arise, enabling us to understand how these structural distortions couple together and give rise to useful technological properties including magnetoelectric and magnetoresistance effects.

[1] Wei-Tin Chen, Chin-Wei Wang, Ching-Chia Cheng, Yu-Chun Chuang, Arkadiy Simonov, Nicholas C. Bristowe & Mark S. Senn, *Nat. Commun.*, **12**, 6319 (2021). [2] Wei-Tin Chen, Chin-Wei Wang, Hung-Cheng Wu, Fang-Cheng Chou, Hung-Duen Yang, Arkadiy Simonov, and M. S. Senn, *Phys. Rev. B*, **97**, 144102 (2018).